

Article

Projected Changes in Spawning Ground Distribution of Mature Albacore Tuna in the Indian Ocean under Various Global Climate Change Scenarios

Sandipan Mondal ^{1,2}, Aratrika Ray ¹, Ming-An Lee ^{1,2,3,*}  and Malagat Boas ¹

¹ Department of Environmental Biology and Fishery Science, National Taiwan Ocean University, Keelung 202, Taiwan; sandipan@mail.ntou.edu.tw (S.M.); 21031006@mail.ntou.edu.tw (A.R.); 11131016@mail.ntou.edu.tw (M.B.)

² Center of Excellence for Oceans, National Taiwan Ocean University, Keelung 202, Taiwan

³ Doctoral Degree Program in Ocean Resource and Environmental Change, National Taiwan Ocean University, Keelung 202, Taiwan

* Correspondence: malee@mail.ntou.edu.tw

Abstract: The present study utilised a geometric mean model in which sea surface temperature, oxygen, and sea surface salinity were used to predict the effects of climate change on the habitats of mature albacore tuna in the Indian Ocean under multiple representative concentration pathway (RCP) scenarios. Data pertaining to the albacore tuna fishing conducted by Taiwanese longline fisheries during the October–March period in 1998–2016 were analysed. The fishery data comprised fishing location (latitude and longitude), fishing effort (number of hooks used), number of catches, fishing time (month and year), and fish weight. Nominal catch per unit effort data were standardised to mitigate the potential effects of temporal and spatial factors in causing bias and overestimation. The Habitat Suitability Index (HSI) scores of potential habitats for mature albacore in the Indian Ocean are predicted to change considerably in response to varying levels of predicted climate change. Under projected warm climate conditions (RCP 8.5), the stratification of water is predicted to cause low HSI areas to expand and potential habitats for mature albacore to shift southward by 2100. The findings derived from these mature albacore habitat forecasts can contribute to the evaluation of potential hazards and feasible adaptation measures for albacore fishery resources in the context of climate change. The distribution trends pertaining to potential habitats for mature albacore should be used with caution and can provide resource stakeholders with guidance for decision-making.

Keywords: arithmetic mean modelling; geometric mean modelling; Habitat Suitability Index; albacore tuna; representative concentration pathway; Indian Ocean



Citation: Mondal, S.; Ray, A.; Lee, M.-A.; Boas, M. Projected Changes in Spawning Ground Distribution of Mature Albacore Tuna in the Indian Ocean under Various Global Climate Change Scenarios. *J. Mar. Sci. Eng.* **2023**, *11*, 1565. <https://doi.org/10.3390/jmse11081565>

Academic Editor: Aurélie Blanfuné

Received: 3 July 2023

Revised: 19 July 2023

Accepted: 6 August 2023

Published: 8 August 2023



Copyright: © 2023 by the authors. Licensee MDPI, Basel, Switzerland. This article is an open access article distributed under the terms and conditions of the Creative Commons Attribution (CC BY) license (<https://creativecommons.org/licenses/by/4.0/>).

1. Introduction

Albacore tuna is one of the most valuable commercial species worldwide. This species, which belongs to the family Scombridae, was first described by Bonnaterre in 1788 and is one of the most commercially exploited fish species [1]. Albacore tuna is consumed in numerous countries [2]. It is a highly migratory species that inhabits the tropical and temperate waters of three oceans, namely the Indian, Pacific, and Atlantic Oceans. It is highly valuable and nutrient-dense and serves as a rich source of lean protein and omega-3 fatty acids. The distribution of albacore tuna in the Indian Ocean varies seasonally. Immature albacore tuna tends to live in the southern part (after 30° S) of the Indian Ocean throughout the year [3] because of the cooler temperature in this region relative to that in the central part of the Indian Ocean. Mature albacore tuna exhibits a similar distribution trend, although this trend can only be observed between April and September [1]. Between October and March, which is the spawning period of albacore tuna in the Indian Ocean, mature albacore tuna migrates northward and live between 10° S and 30° S [1,4]. Thus, this

area, where the sea surface temperature (SST) is warm, is considered the spawning ground of albacore tuna in the Indian Ocean.

The distribution pattern of mature albacore tuna in the Indian Ocean can be determined using SST. In addition to SST, oxygen (OXY), sea surface salinity (SSS), and sea surface height (SSH) are major factors that affect the habitats of albacore tuna. Each of these factors also uniquely influences various aspects of the lives of mature albacore or albacore tuna. For example, SST can directly or indirectly influence numerous aspects of the lives of ocean fish species, such as their metabolic rate, reproduction, spawning behaviour, activity level, disease development, stress, and OXY consumption. SST also affects the migratory behaviours of highly migratory fish, such as albacore tuna, because such behaviours occur in response to specific temperature gradients [5–7]. For mature or spawning albacore, spawning time, egg development and incubation, and larval survival and growth are highly dependent on SST [8]. OXY level also plays a key role in several aspects of the lives of fishes, including their respiration, survival, growth, activity level, behaviour, and reproduction [9]. For mature or spawning albacore, gamete development and hormonal regulation are highly dependent on OXY level [10]. SSS also affects several major aspects of the lives of fishes, such as osmoregulation [11], migration [12], and spawning [13]. Sperm activation, egg fertilisation, and embryo development are highly dependent on SSS [14]. SSH influences water circulation and exchange in coastal regions, which can affect salinity levels and water quality [15]. Higher sea levels can increase tidal cleansing and water circulation, which may improve water quality and salinity [16]. For mature or spawning fishes, SSH can influence the effectiveness of their spawning and reproduction activities [17]. Changes in SSH may disrupt the timing, duration, and location of reproduction, thereby affecting the recruitment and abundance of fish populations [18]. The aforementioned findings highlight the relevance of individual oceanographic variables to mature albacore tuna.

Numerous oceanographic variables are highly dependent on SST and change drastically with SST. For example, SST can affect the metabolic rates of various marine organisms. In general, a higher SST increases the metabolic demand for OXY, which increases OXY consumption rates. This phenomenon can deplete OXY levels in the water, especially in regions with high biological activity or during periods of low circulation [19]. SST also influences the rate of ocean surface evaporation and the quantity of precipitation over the ocean. A higher SST tends to increase evaporation, resulting in increased salt concentration and SSS. By contrast, a lower SST can reduce evaporation and SSS. Changes in SST can also affect atmospheric circulation patterns, modifying precipitation rates and, consequently, SSS [20]. Such changes can affect seawater density; warmer water is less dense than cooler water, which causes it to rise and contribute to an increase in SSH, whereas cooler water is denser and sinks, resulting in a decrease in SSH. In coastal areas and regions influenced by upwelling or downwelling processes, such vertical movements of water masses, which are driven by density, can be observed [21]. The aforementioned facts indicate that the habitat of mature albacore tuna and other aspects of their lives that are related to SST, OXY, SSS, and SSH are altered when SST changes.

Globally, the effects of human activities and environmental pollution on fish stocks and marine ecosystems are substantial. Human activities such as overfishing (decline in fish stocks), bottom trawl and dynamite fishing (habitat destruction), industrial discharge (environmental pollution), bycatch (catching endangered, juvenile fishes), illegal fishing (overfishing), etc. effect the fish stock and the ecosystem adversely [22,23]. Fish stocks and aquatic ecosystems can suffer severe and negative effects as a result of environmental pollution [24]. Fishes are extremely sensitive to environmental changes, and pollution can affect their ability to reproduce, find a suitable home, and maintain general health [25]. This is because environmental pollution leads to water quality degradation, habitat destruction, ocean acidification, eutrophication, etc. In addition, global climate change caused by higher greenhouse gas emissions has led to a drastic increase in the global temperature relative to that of the previous decade [26]. Since the Industrial Revolution [27], human activities have led to substantial increases in the concentrations of numerous greenhouse

gases, particularly CO₂, that have caused an increase in SST. This increase is due to oceans absorbing and storing heat from the atmosphere [28]. Because of its high heat capacity, seawater can absorb and retain a considerable amount of heat, and the oceans function as a heat sink under conditions of global temperature increases [29], which contributes to SST warming. An increased SST can initiate feedback mechanisms that contribute to further increases in temperature levels [30]. When SST increases, the melting of sea ice and glaciers accelerates, which reduces the Earth's albedo (i.e., reflectivity), causes the oceans to absorb more heat, and enhances the heating effect. Globally, ocean SST is predicted to increase by 1 °C–4 °C by 2100. Numerous oceanographic variables, which are strongly associated with SST, are also changing, which may result in changes to the habitats of albacore tuna [31]. Several studies have revealed that such changes are occurring in the oceans [32–34]. For example, the summer feeding season in the Nordic Seas witnessed a significant geographical expansion of mackerel from 2007 to 2016. This expansion was primarily influenced by the growing size of the mackerel stock, while being limited by the availability of suitable temperature habitats preferred by the species [35]. Another study unequivocally establishes sea temperature as the principal determinant of fish community composition within the Northeast Atlantic continental shelf. This study strongly suggests that fishes located at higher latitudes will experience the greatest degree of impact as a result of ongoing climate change [36].

The marine science community has studied likely climate change scenarios under various representative concentration pathway (RCP) conditions to make qualitative and quantitative projections of marine ecosystem responses to atmospheric changes [37,38]. RCPs are used to characterise an extensive range of greenhouse gas outflow scenarios, including a rigid relief scenario (RCP 2.6; [39]), a moderate scenario (RCP 4.5; [40]), and an exceptionally high GHG-outflow scenario (RCP 8.5; [41]). On the basis of the aforementioned findings, the present study hypothesised that the spawning ground distribution of Indian Ocean mature albacore tuna changes with the global climate change scenario that is considered. The present study assessed the changes in the spawning ground distribution of mature albacore tuna in the Indian Ocean in response to changes in SST and other related oceanographic variables under various RCP scenarios.

2. Materials and Methods

2.1. Albacore Tuna Fishery Data

Albacore tuna fishery data were collected from a journal containing records of the large-scale, longline fishing activities (deep water fishing involving a boat with a gross register tonnage of >100 tonnes and length of >24 m) of Taiwanese fisheries during January–December in 1998–2016; the journal was obtained from the Overseas Fisheries Development Council of Taiwan. Data pertaining to small-scale fishing activities (primarily coastal water fishing involving a boat with a gross register tonnage of <100 tonnes and length of <24 m) were not used in this analysis because such data corresponding to the study period (1998–2016) were lacking. The spatial extent of the collected data was 0° S to 45° S and 20° E to 120° E (spatial resolution = 1° × 1°). The collected logbook information included the year, month, latitude, longitude, number of catches, number of hooks used, number of hooks used per basket (not available for all years), and weight (type of weight [dry or moist] was not specified). Notably, the data set lacked information on soaking time, connection depth, and operation time. The first maturity weight of albacore tuna in the Indian Ocean is 14 kg [4]. The present study set the average weight of 14 kg as the threshold for distinguishing between mature and immature albacore; that is, albacore tuna with an average weight of >14 kg were regarded as mature. Albacore tuna in the Indian Ocean primarily spawn in the western and central regions of the Indian Ocean, that is, in areas such as the Mozambique Channel, the waters surrounding Madagascar, and the Southwest Indian Ocean [1]. The region between 10° S and 30° S is the primary spawning ground for albacore tuna in the Indian Ocean, and they primarily spawn there in

October–March [1,4]. The present study selected and used fishing data pertaining to the fishing activities conducted between 10° S and 30° S and between October and March.

2.2. Oceanographic Data

In the present investigation, data related to four oceanographic parameters were collected (Table 1). The spatial resolution of the data, which pertained to fishing activities conducted between 10° S and 30° S and between 20° E to 120° E, varied. All collected data pertained to the fishing activities conducted during October–March in 1998–2016. Because the spatial resolution of the fishery data was 1° × 1°, Matlab version 2019a was used to interpolate the collected oceanographic data to a 1° × 1° grid to ensure they matched the spatial coverage of the fishery data.

Table 1. Analysed oceanographic parameters.

Environmental Data	Abb.	Unit	Source	Time Period	Spatial Resolution	Temporal Resolution
Sea surface temperature	SST	°C	COP	1998–2016	0.08° × 0.08°	Monthly
Dissolved oxygen	OXY	mL/L				
Sea surface salinity	SSS	psu				
Sea surface height	SSH	m				

Abbreviation: COP, Copernicus (<https://resources.marine.copernicus.eu/products> (accessed on 14 November 2021)).

2.3. Projected Oceanographic Data

All oceanographic projection data were collected from the Intergovernmental Panel on Climate Change (IPCC) climate models that were tested under the RCP 2.6, 4.5, and 8.5 scenarios. Data on the environmental variables were downloaded from the Earth System Grid Federation. To minimise the risk of significant bias resulting from the use of a single climate model, the average result derived from multiple climate models was used in accordance with the recommendations of the IPCC (Table 2). The projection data were those for October–March in the years 2040, 2070, and 2100, and this study focused on the short-, middle-, and long-term effects of projected climate-related changes on the distribution pattern of mature albacore during spawning months under all RCP scenarios. The data from all considered climate models were interpolated to a 1° × 1° spatial grid by using Matlab version 2019a because the collected fishery data were interpolated to a 1° × 1° spatial grid.

Table 2. Sources of oceanographic projection data corresponding to various climate models.

Institute	Code	Resolution
Institute Pierre Simon Laplace	IPSL	1° × 1°
Geophysical Fluid Dynamics Laboratory	GFDL	0.3–1° × 1°
Commonwealth Scientific and Industrial Research Organization	CSIRO	1.5° × 1°
Hadley Center Global Environment Model	HadGEM	0.3–1° × 1°
Max Plank Institute for Meteorology	MPI	1° × 1°
Canadian Earth System Model	CanSEM	1.5° × 1°

2.4. Standardisation of Nominal Catch per Unit Effort

Mature albacore relative abundance was indexed as nominal catch per unit effort (*N.CPUE*). *N.CPUE* (per 1000 hooks) was calculated using the following formula:

$$N.CPUE = \frac{\text{No. of albacore catch}}{\text{No. of hooks used}} \times 1000 \tag{1}$$

To minimise the influence of spatial (latitude, longitude) and temporal (year, month) variables, the obtained *N.CPUE* data were standardised by applying generalised linear models (GLMs), which are widely recognised as a means of obtaining filtered and unbiased standardised catch per unit effort (S.CPUE) values. The GLMs were constructed using multiple explanatory variables in R-Studio version 3.6.0. The GLMs were formulated as follows:

$$GLM_n : \text{Log}(N.CPUE + c) \sim \text{Year} + \text{Month} + \text{Latitude} + \text{Longitude} + \text{Interactions} \quad (2)$$

where *c* is a constant value of 0.1, *n* is the number of variables, *GLM_n* is a model with *n* factors, and μ is the interactions of factors (*Year* × *Latitude*, *Year* × *Longitude*, and *Latitude* × *Longitude*). The obtained S.CPUE results were used in subsequent analyses.

2.5. Species Distribution Modelling

Two methods were employed to complete species distribution modelling, namely arithmetic mean modelling (AMM) and geometric mean modelling (GMM). These two methods are widely used to identify suitable habitats for species. A suitable habitat is an environment or area that meets the basic requirements for an organism or species to survive, reproduce, and grow. A habitat’s suitability is determined by whether it has the temperature, humidity, food availability, shelter availability, and other resources that an organism requires to survive. The subsequent subsections describe the techniques employed in the current study for species distribution modelling.

2.5.1. Construction of Suitability Index Curves

Smoothing spline regression was used to determine the relationships between the relative abundance of mature albacore tuna and their oceanographic preferences [42] and those between S.CPUE and various oceanographic variables. S.CPUE was considered a dependent variable in regression analysis, and all selected oceanographic parameters were considered explanatory variables. The suitability index (*SI*) curve for mature albacore tuna was obtained by considering S.CPUE and all oceanographic variables, and the curve was subsequently normalised using the following formula [43]:

$$SI = \frac{Y - Y_{min}}{Y_{max} - Y_{min}} \quad (3)$$

where *Y_{max}* and *Y_{min}* are the maximum number and minimum number of S.CPUE or oceanographic variable observations, and *Y* is the simulated (predicted) value from *Y_{max}* to *Y_{min}*; *SI* values range from 0 to 1.

SI values were calculated using the summed frequency distribution of the S.CPUE of each class, and the *SI* values were assumed to range between 0 and 1. The midpoint of the class interval of each environmental variable was used as the observed value for *SI* model fitting. Finally, the relationships between the *SI* and oceanographic variable results were determined using the following formula [44–46]:

$$SI = e^{\alpha(m+\beta)^2} \quad (4)$$

where *m* denotes the response variable (oceanographic variables), and α and β are fixed by applying the nonlinear least squares estimate to minimise the residual between an *SI* observation and the *SI* function.

2.5.2. Model Construction

AMMs and GMMs were constructed using the *SI* values by employing the following formulas:

$$AMM = (SI_1 + SI_2 + SI_3 + \dots + SI_n)/n \quad (5)$$

$$GMM = (SI_1 \times SI_2 \times SI_3 \times \dots \times SI_n)^{(1/n)} \tag{6}$$

where SI_1, SI_2, SI_3 are the observations and n is the n th observation of the SI . Various parameter combinations were applied using AMM and GMM. The results obtained using these combinations were analysed using R-Studio version 3.6.0.

2.6. Model Selection and Prediction

From among the models derived using AMM and GMM, one model was selected on the basis of the Akaike information criterion (AIC; i.e., the least value is optimal) and adjusted R-squared (i.e., the highest value is optimal) values. For the validation of the selected model, the fishing data set was randomly divided into two parts, with 70% of the data used for training and 30% used for testing. The Pearson correlation coefficients and areas under the curve (AUCs) were calculated for both the training and testing data sets. The data set that exhibited the least difference between its training and testing sets in terms of R and AUC values was selected as suitable for minimising the bias (70:30) of the model. This data set was subsequently used to obtain predictions. The predicted values for each point of the study area from the final model were then mapped to a $1^\circ \times 1^\circ$ spatial grid by using ArcGIS software (version 10.2).

3. Results

3.1. Standardisation of N.CPUE Data

The final GLM model, which included all factors, had a deviance explained value of 0.58 (Table S1). Because the standardisation model's histogram and quantile–quantile plot (Figure 1) revealed a nearly normal distribution, the model was used to standardise the mature albacore tuna $N.CPUE$. The monthly summed catch per unit effort (CPUE) ranged from 0.1 to 2700 individuals (Figure 2). After standardisation, the summed monthly CPUE decreased to a range of 0.1 to 1700 individuals. The S.CPUE was used as a metric for analysing the mature albacore tuna data.

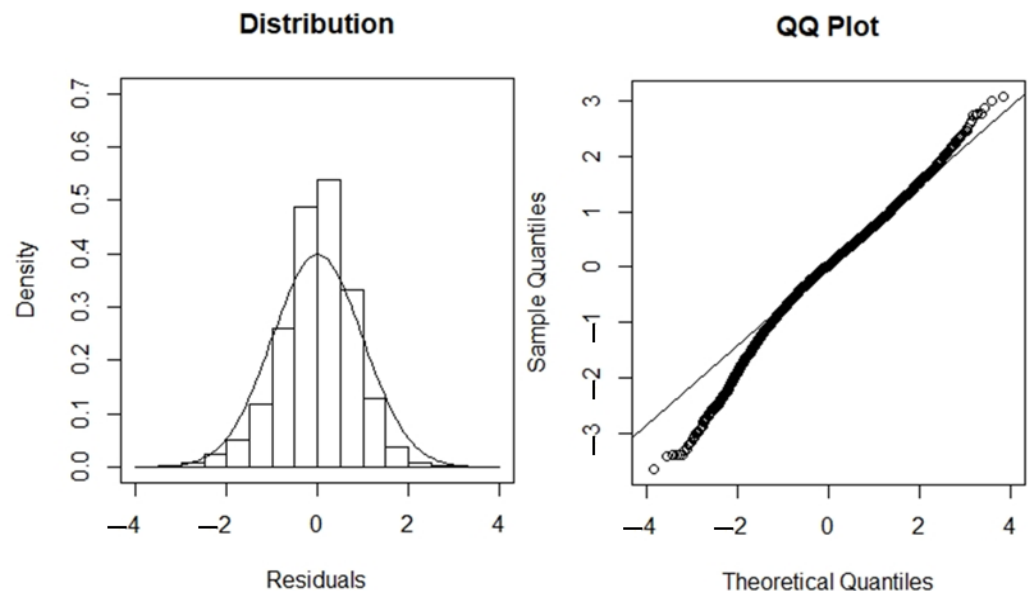


Figure 1. Residual distribution and QQ plot for selected GLM for mature albacore tuna.

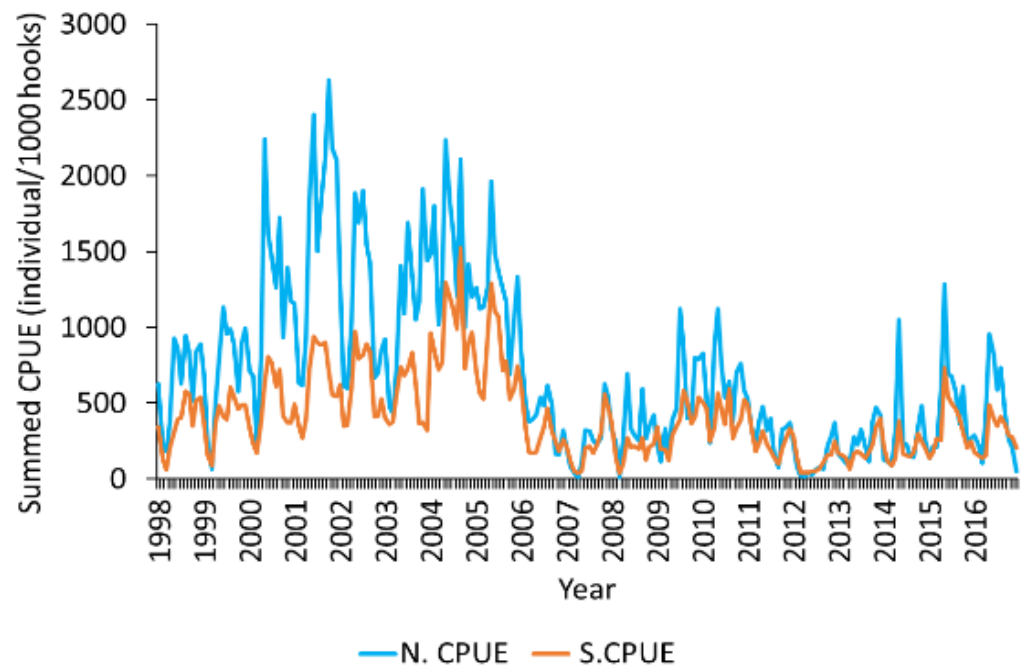


Figure 2. Comparison of *N.CPUE* and *S.CPUE* results based on selected GLM for mature albacore tuna.

3.2. Construction of *SI* Curves

SI curves for mature albacore tuna were generated on the basis of various selected parameters. Subsequently, Habitat Suitability Index (HSI) scores were calculated. The optimal ranges for SST, SSS, OXY, and SSH were determined to be 25–29 °C, 34.85–35.55 psu, 5–5.3 mL L⁻¹, and 0.5–0.7 m, respectively, under the condition of the *SI* value being >0.6. When the *SI* value was >0.6, the *S.CPUE* for mature albacore tuna in the Indian Ocean during October–March was highly correlated with SST (predominant value = 27.5 °C), SSS (predominant value = 35.05 psu), OXY (predominant value = 5.1 mL L⁻¹), and SSH (predominant value = 0.55 m; Figure 3). Subsequently, *SI* curves were plotted using the smoothing spline technique.

3.3. Analysis of Habitat Models, Model Selection, and Validation

Table 3 presents the results obtained using AMMs and GMMs when the selected parameters were used in all feasible combinations. The AMM-designated model 2, which incorporated OXY and SSS results, exhibited superior performance relative to the other models. An analysis revealed that the model had a minimum AIC value of 14.240 and maximum adjusted R-squared value of 0.845, and therefore, model 2 was considered to be the most suitable AMM. Among the GMMs, model 7 (GMM_7) with the combination of OXY, SST, and SSS had the most favourable performance; it had the highest adjusted R-squared value (0.87) and lowest AIC value (18.943) and was therefore selected as the optimal model.

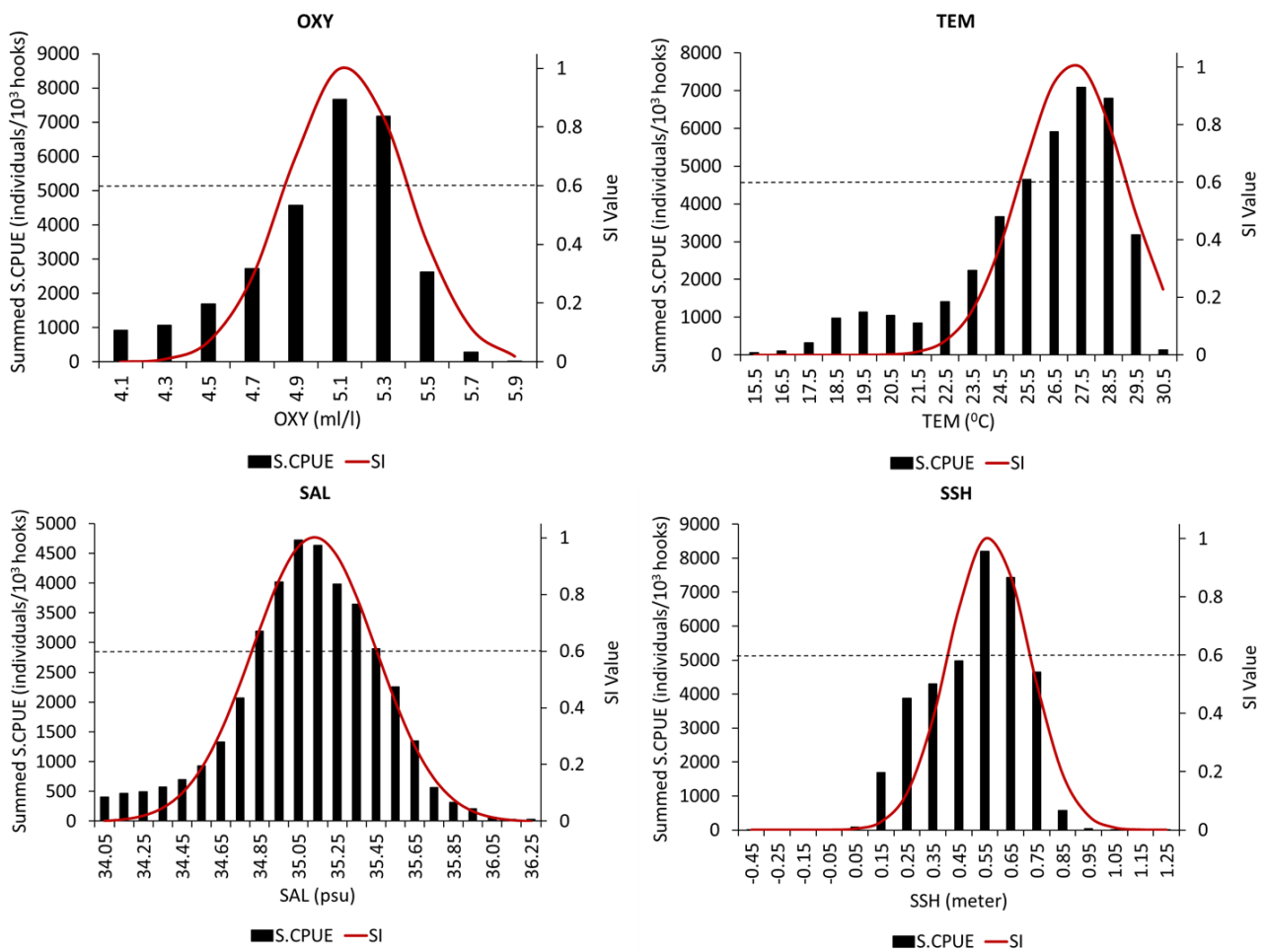


Figure 3. SI curves of selected environmental variables pertaining to mature albacore tuna during October–March (plotted using smoothing spline regression). The black bars, black dotted lines, and red solid lines indicate the summed S.CPUE, SI scores with a cut-off value of >0.6, and SI curves, respectively. The intersections of the horizontal dotted lines and SI curves indicate the optimal environmental range of each parameter.

Table 3. Performance of AMMs and GMMs for mature albacore tuna (October–March). Bolded and colour-marked values indicate optimal AMM and GMM results, respectively.

No.	Model	AMM				GMM			
		a	b	AIC	Adj. R2	a	b	AIC	Adj. R2
1	OXY, SST	0.535	4.995	37.015	0.507	1.854	3.692	25.753	0.693
2	OXY, SSS	−0.661	5.721	14.240	0.845	1.494	3.423	24.822	0.679
3	OXY, SSH	−0.391	5.27	22.646	0.836	2.006	2.619	26.393	0.501
4	SST, SSS	2.595	−2.129	26.758	0.375	1.144	−0.77	26.186	0.115
5	SST, SSH	1.788	−0.456	31.624	0.1	0.85	0.882	25.864	0.022
6	SSS, SSH	−0.23	3.096	26.450	0.59	−0.31	3.379	23.907	0.694
7	OXY, SST, SSS	−0.896	5.623	33.347	0.71	1.258	4.459	18.943	0.87
8	OXY, SST, SSH	0.801	3.272	40.487	0.239	1.464	4.074	24.942	0.751
9	SST, SSS, SSH	2.117	−0.361	38.593	0.117	0.339	2.273	29.604	0.333
10	OXY, SST, SSS, SSH	0.725	3.25	41.974	0.2	1.06	4.5	20.545	0.853

3.4. Validation of Selected Models

GMM_7 was evaluated using four validation techniques, all of which indicated minimal differences in the coefficient values (R and AUC) between the split data sets (70:30). This result indicates that the predictive performance of GMM_7 was not affected by significant bias (Table 4). Therefore, GMM_7 was employed to generate an overall HSI forecast for all sampling sites within the study area.

Table 4. Validation results for GMM_7 before HSI prediction.

Techniques	70%		30%	
	R ²	AUC	R ²	AUC
Random split	0.845	0.872	0.839	0.865

3.5. HSI Prediction

In the month of October, the zones with high S.CPUE were scattered throughout the study area. For the months of November to February, the zones with high S.CPUE for mature albacore tuna were mainly between 10° S and 25° S (Figure 4). From February onward, a southward shift occurred. In February, a high S.CPUE zone was noted at approximately 15° S. In March, this shift became more pronounced. A zone with a very low S.CPUE appeared between 10° S and 25° S and at approximately 35° S. The predicted HSI (P.HSI) of this zone was in line with the S.CPUE trend. Longitudinally, this zone started extending eastward and up to 100° E in the month of March. The P.HSI results for October–March indicated that a suitable habitat zone was mainly formed between 10° S and 25° S (Figure 4).

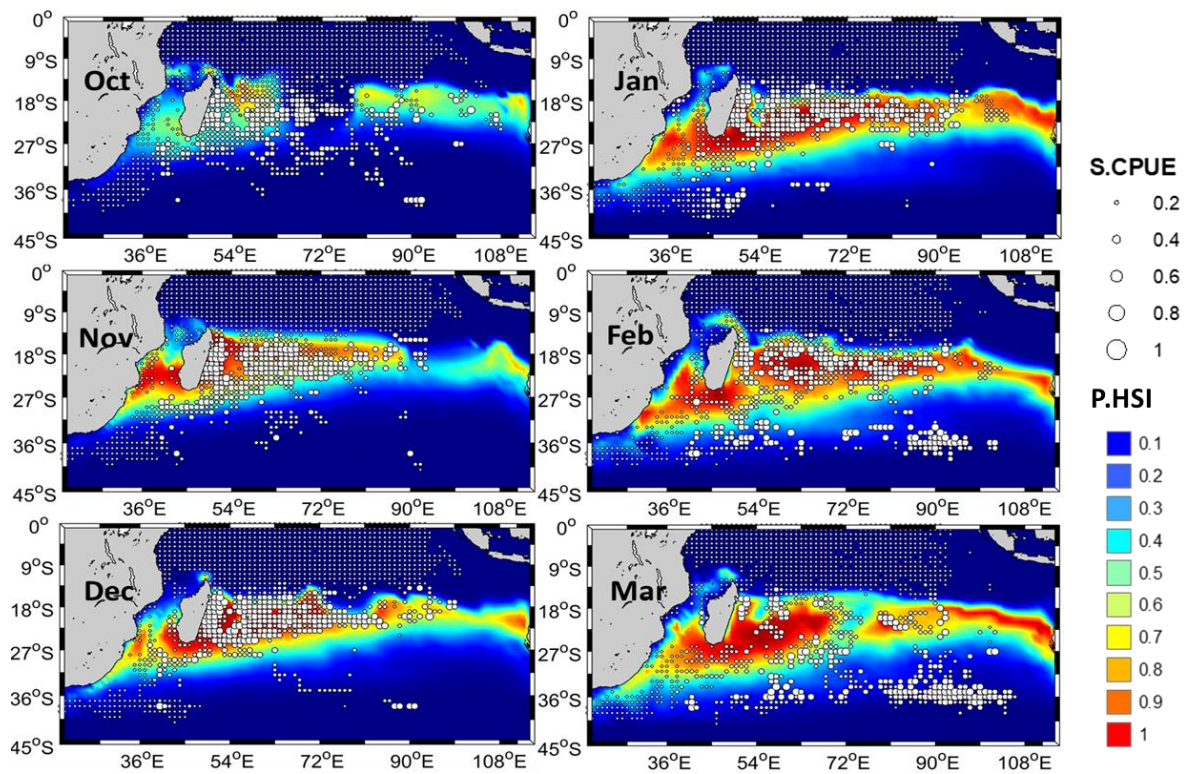


Figure 4. Monthly spatial distribution (October–March) of average S.CPUE for mature albacore tuna in the Indian Ocean mapped onto monthly P.HSI in 1998–2016.

3.6. Projected Habitat Changes

Figure 5 presents the changes in the HSI scores for mature albacore tuna during October–March under various RCP scenarios and at various time points. A high HSI (>0.6) zone was identified between 15° S and 30° S. The predicted latitudinal pattern of the high HSI zone for the year 2040 was nearly identical to that for the year 2016 under all RCP scenarios. For the year 2070, the high HSI zone was situated between 20° S and 30° S under the RCP 2.6 and 4.5 scenarios. The high HSI zone exhibited a slight southward shift in the year 2070. At the end of the year 2100, the high HSI zone remained situated between 25° S and 35° S under the RCP 2.6 and 4.5 scenarios. However, a clear change occurred under the RCP 8.5 scenario; the high HSI zone exhibited a notable southward shift, crossing 35° S in the year 2100 under the RCP 8.5 scenario. Two high HSI zones were identified; one was situated between 20° S and 25° S and 90° E and 100° E, and the other was situated between 25° S and 35° S and 30° E to 40° E.

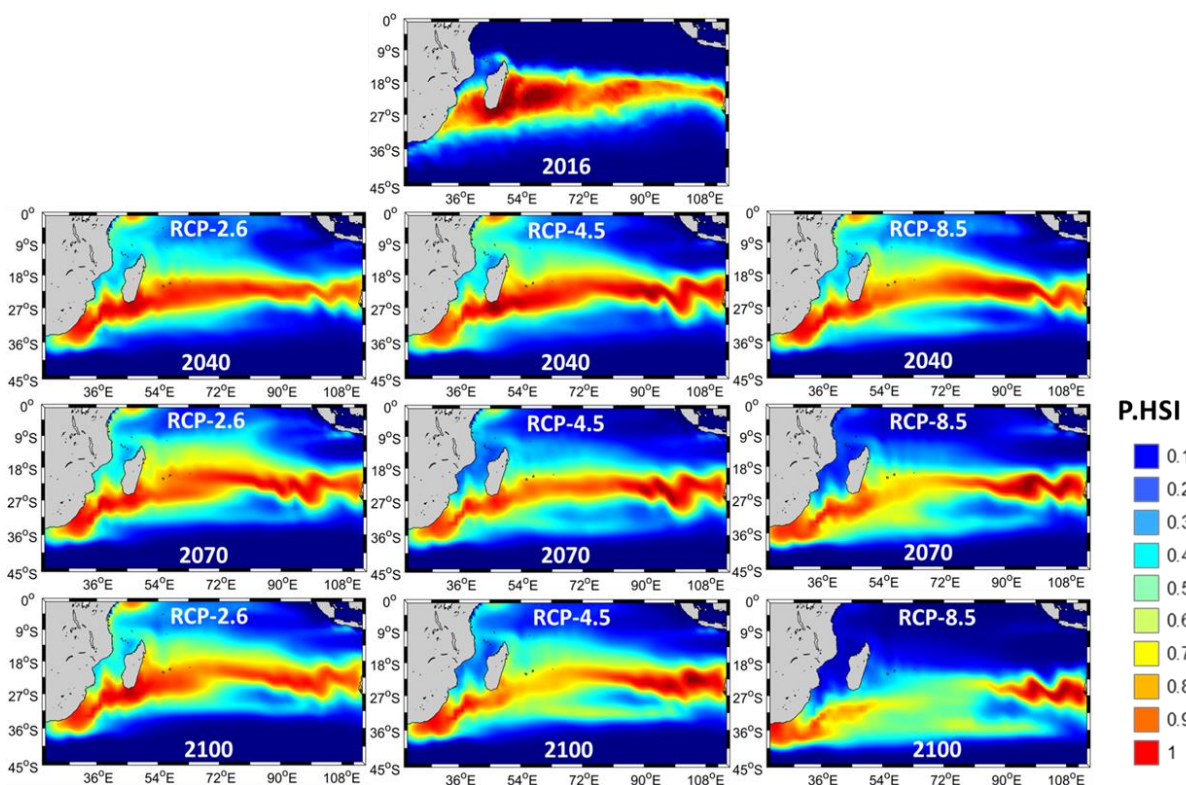


Figure 5. Changes in ensemble HSI for mature albacore tuna during October–March under various RCP scenarios and at various time points.

Figure 6 presents the results pertaining to the latitudinal shift in the ensemble HSI score for mature albacore tuna during October–March under various RCP scenarios and at various time points. For the year 2016, the high HSI zone was situated between 18° and 25° S. Under the RCP 2.6 scenario, this zone exhibited a high HSI trend that was mostly similar to that for the year 2016 at three time points; the HSI scores ranged between 0.5 and 0.6. Under the RCP 4.5 scenario, this zone exhibited a high HSI trend that was mostly similar to that for the year 2016 at three time points; the HSI scores were slightly greater than 0.5. In terms of changes that occurred when both scenarios (2.6 and 4.5) and time points (2040, 2070, and 2100) were considered, the HSI score only exhibited a considerable reduction after 25° S. Under the RCP 8.5 scenario, the high HSI zone exhibited a substantial latitudinal shift for the years 2040 and 2070, and the HSI score changed slightly relative to that for the year 2016. However, for the year 2100, the HSI score decreased to nearly 0.4, and the high HSI zone was situated between 25° S and 35° S, indicating an upward latitudinal shift. For the year 2100, the HSI score of the area between 18° S and 25° S was

slightly less than 0.4 under the RCP 8.5 scenario, which is lower than the values obtained under the RCP 2.6 (0.5–0.6) and 4.5 (0.5–0.6) scenarios. This finding indicates a notable shift in the high HSI zone is likely to occur in the year 2100 under the RCP 8.5 scenario. Figure 7 represented the latitudinal changes of the 27.5 °C isotherm line under various climate change scenarios.

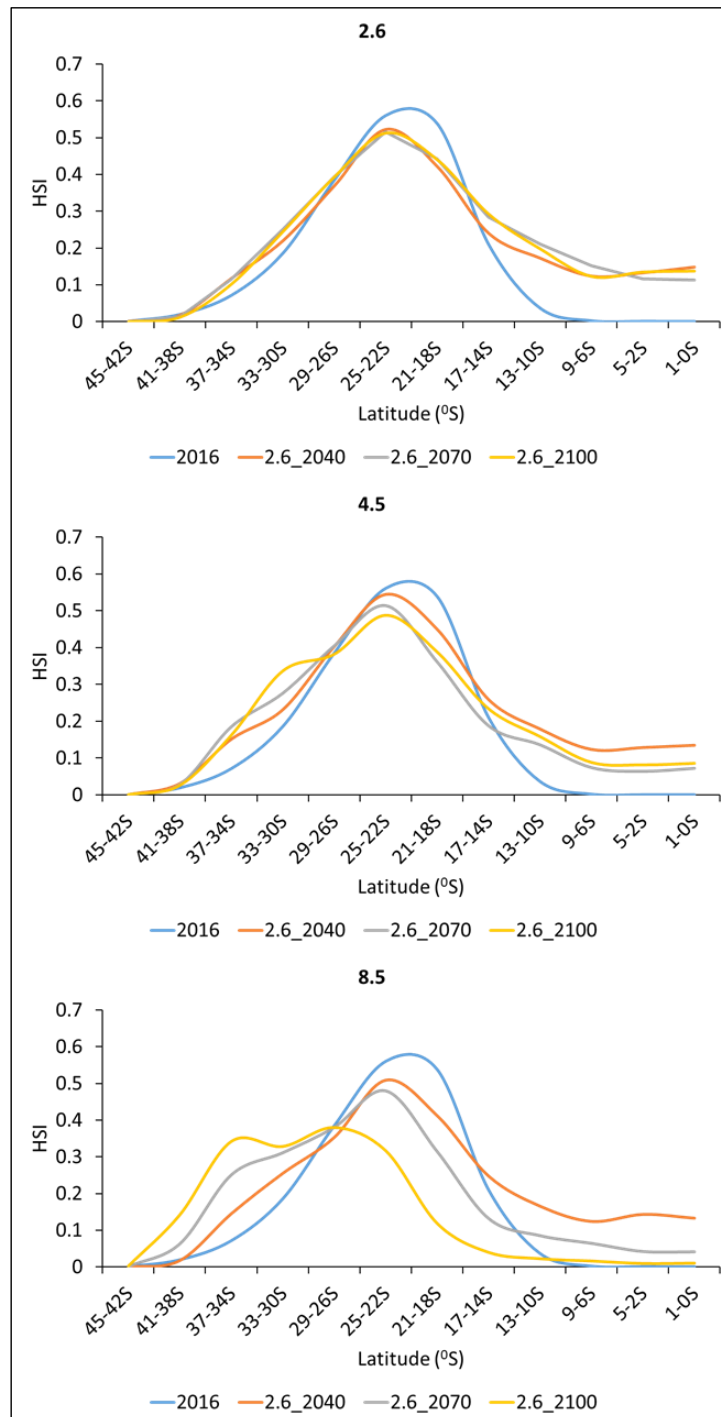


Figure 6. Latitudinal shift of ensemble HSI score for mature albacore tuna during October–March under various RCP scenarios and at various time points.

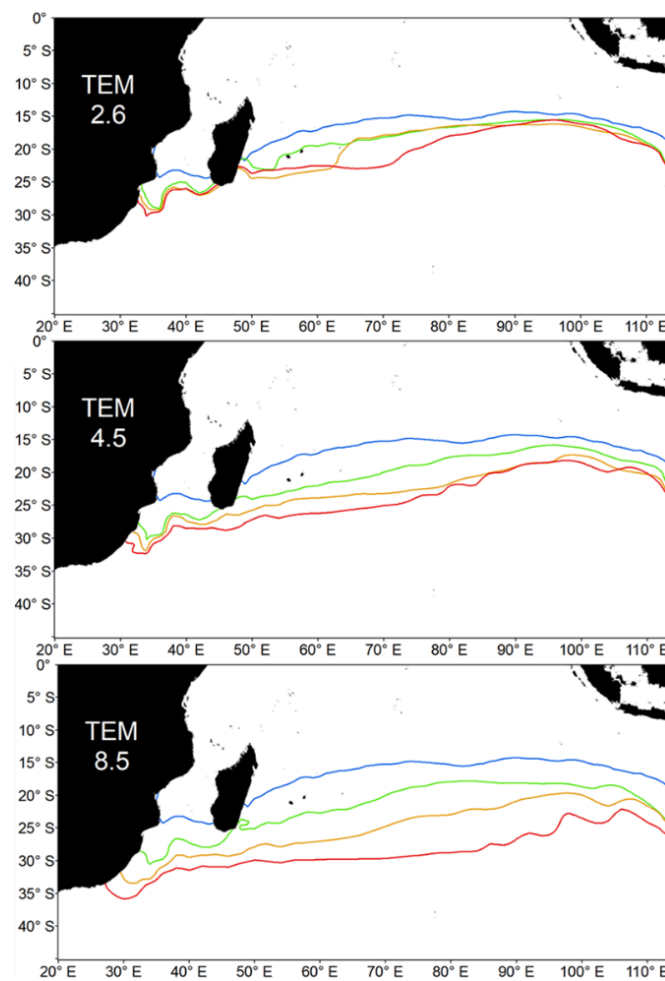


Figure 7. Latitudinal changes of the 27.5 °C isotherm line under various climate change scenarios (red, 2016; yellow, 2040; green, 2070; blue, 2100).

4. Discussion

4.1. Projected Habitat Changes under Various Climate Change Scenarios

Scholars reported major shifts in the distribution of marine organisms in the global ocean due to anthropogenic climate change [47]. Our findings indicate that the suitable habitat for mature albacore tuna is likely to shift in the future. Our prediction results, especially those for the RCP 8.5 scenario, indicate that the suitable habitat for mature albacore tuna will undergo a size reduction and bifurcation (Figure 5). For the year 2016, the high HSI zone for mature albacore tuna during October–March was situated mainly between 15° S and 25° S; however, for the year 2100, the zone crossed 35° S under the RCP 8.5 scenario, indicating the zone shifted southward. Under the RCP 8.5 scenario, which is an extreme and worse-case scenario with respect to climate change, the suitable habitat for mature albacore tuna shifted toward higher latitudes (Figure 6). This finding is consistent with the predicted changes in the natural habitats of South Pacific albacore tuna [48]; albacore tuna in the Northeast Pacific [49]; Atlantic tunas, such as bluefin tuna [50]; and other fish species, such as billfishes and mackerels.

4.2. Increased Water Temperature and Albacore Spawning

Climate change poses a threat to pelagic predators such as tuna [51]. Latitudinal variations in the optimal SST range for albacore tuna may cause a habitat shift (Figure 7). Climate change substantially affects the circulation of wind and water in the ocean, which can lead to changes in upwelling and downwelling processes that affect the availability of

OXY and nutrients. Mature albacore tuna living outside of their preferred SST range may be at risk of local or global extinction if they cannot migrate or compete for resources. In the current study, the optimal SST for mature albacore tuna during October–March was determined to be $>27^{\circ}\text{C}$. This phenomenon can be attributed to the spawning behaviour of fully-grown albacore tuna during these months, which leads to them engaging in less swimming activity. Thus, despite the decrease in continuous activity, energy loss decreases even at high temperatures. Mature albacore tuna tends to prefer warm temperatures during their spring spawning period because such temperatures enable them to regulate their body temperature and manage heat loss. Mature spawning albacore tuna were observed by Chen et al. (2005) [4] in seas with a temperature of $>27^{\circ}\text{C}$, and temperature and food availability were reported to be linked to fish distribution constraints [46]. An SST that is higher than the optimal range may hinder the reproductive development of mature albacore tuna by affecting their muscle contraction speed, disrupting their energy expenditure, reducing their performance, increasing their stress susceptibility, and impeding their growth.

4.3. Temperature and Other Oceanographic Parameters

Temperature acclimatisation incurs an energetic expense that affects numerous physiological functions of fishes (e.g., reproduction, growth, foraging, and swimming) that are significantly associated with oceanographic drivers. To optimise biological efficiency and minimise physiological adjustment costs, albacore tuna may migrate to habitats with suitable temperatures with habitat heterogeneity [52]. Albacore tuna becoming capable of migrating to and locating dynamic optimal environments that are beyond their present distribution can lead to changes in their engagement in fishing activities, which may also be influenced by prey movements. Elevated temperatures have a negative effect on OXY solubility, which is also influenced by salinity. Increases in temperature and salinity lead to a decrease in OXY solubility [53], which impairs fish growth. Although jellyfish can thrive in low-OXY waters, albacore tuna, which expend more energy, cannot. Albacore tuna tend to move to shallow oceans with more dissolved OXY. Low ($>2\text{--}4\text{ mg L}^{-1}$) to hypoxic ($>0\text{--}2.0\text{ mg L}^{-1}$) concentrations of dissolved OXY may stress and kill albacore tuna, and therefore, ocean OXY loss may affect albacore tuna distribution. Acidification may also limit the optimal temperature range for albacore tuna, which because of ocean warming, may reduce the number of suitable spawning habitats for such tuna and lead to a decrease in larvae survival rates. This effect may be further intensified in environments with low concentrations of dissolved OXY and lead to a further reduction in larvae survival rates [54]. An increase in seawater salinity leads to an increase in seawater density. Additionally, the salinity of seawater influences the correlation between temperature and density [55] and thereby influences oceanic precipitation and evaporation. Changes in SSS affect the osmoregulatory expenditure of albacore tuna. A disparity between environmental salinity and the internal osmotic concentration of a marine fish species can result in either a loss or gain of salt and water. Consequently, deviations from the preferred SSS range for albacore tuna may prompt them to migrate to areas with more favourable salinity conditions. SSS also indirectly affects ALB abundance by influencing prey distribution and availability. SSH affects the physical habitat of pelagic species in the open ocean. Positive and negative SSH anomalies affect the formation of eddies and gyres, respectively, which delineate the areas of convergence and divergence where tuna prey may congregate. The frontal systems of gyres can attract tunas [56], and albacore tuna prefer slightly negative or positive SSH levels [57].

Understanding the habitat preferences of albacore tuna is crucial, and the factors that contribute to a high CPUE in a given area must be clarified. The present study identified the latitudinal shifts in the centre of gravity of suitable habitats to determine the habitat shift patterns of albacore tuna. This study's analysis of longitudinal changes in the centre of gravity of such habitats provides valuable insight into such patterns. The findings of the present study reveal that the HSI scores for albacore tuna are likely to decline considerably

in regions in which they have generally been high. The present study focused on a specific set of parameters; understanding the effects of other parameters is crucial for improving HSI scores. A key challenge in studying such parameters to identify potential shifts in distribution is the accessibility of data on oceanographic and biological variables that can be incorporated into climate models. Thus, future studies should determine how changes in the growth, reproduction, and survival rates of albacore tuna affect their distribution.

4.4. Sustainable Development Goals

Our findings reveal that climate change affects the spawning habitat structure of mature albacore tuna in the Indian Ocean. When applied in an appropriate context, habitat or spatial distribution modelling can assist albacore tuna management by solving maritime environmental problems. For example, such modelling can be employed to identify underused fishing locations [58]. Increasing the ease with which fishing site identification can be completed would lead to a higher fishery income and reduce the effort, trip times, fuel consumption, and expenses of fishing. Nevertheless, fishery managers must remain conscious of the United Nations' Sustainable Development Goals (SDGs) because easier identification of fishing sites may lead to a greater risk of overfishing [59]. SDG 14 has increased global awareness of the relevance of ocean health to the planet's future [60], and its key focus is conservation [61]. Habitat modelling can assist conservation of overexploited habitats because it can be employed to determine the distribution zone of a given species. Stock evaluations of high or low catch zones can be conducted to detect overexploitation or under exploitation [62]. The main objectives of SDG 14 include addressing overfishing, climate change, and the unique positions of less-developed countries and small island states [63] through institutional support. SDG 14.4 indicates that maintaining biologically viable fish stocks should be prioritised, and identifying shifts in the spawning habitats of albacore tuna under various climate change scenarios can contribute to the achievement of this objective. To enhance stock sustainability, highly exploited regions should be protected through the imposition of temporary fishing bans and provision of overfishing subsidies. To combat overfishing, fishing vessel subsidies for less-exploited regions should be withdrawn. Scientific research and marine technology transfers may also provide support for efforts toward ensuring ocean sustainability. The aforementioned points highlight the relevance of the present study, in which habitat modelling was performed under various global climate change scenarios; this study represents a step toward ensuring the long-term sustainability of mature albacore tuna stocks in the Indian Ocean.

Supplementary Materials: The following supporting information can be downloaded at: <https://www.mdpi.com/article/10.3390/jmse11081565/s1>, Table S1. Performance of different combinations of GLM models for the standardization of mature albacore nominal CPUE.

Author Contributions: Conceptualisation, S.M. and M.-A.L.; methodology, M.-A.L. and S.M.; software, S.M.; validation, M.-A.L.; formal analysis, S.M.; investigation, M.-A.L.; resources, M.-A.L.; writing—original draft preparation, S.M. and A.R.; writing—review and editing, M.-A.L. and M.B.; visualisation, M.-A.L. All authors have read and agreed to the published version of the manuscript.

Funding: This study was funded by the National Science & Technology Council of Taiwan with grant numbers NSTC 111-2923-M-019-001-MY2 and NSTC 111-2811-M-019-011.

Data Availability Statement: For accessing the data please contact to the following email: malee@mail.ntou.edu.tw.

Conflicts of Interest: The authors declare no conflict of interest.

References

1. Nikolic, N.; Morandeau, G.; Hoarau, L.; West, W.; Arrizabalaga, H.; Hoyle, S.; Nicol, S.J.; Bourjea, J.; Puech, A.; Farley, J.H.; et al. Review of albacore tuna, *Thunnus alalunga*, biology, fisheries and management. *Rev. Fish Biol. Fish.* **2017**, *27*, 775–810. [CrossRef]
2. Guillotreau, P.; Squires, D.; Sun, J.; Compeán, G.A. Local, regional and global markets: What drives the tuna fisheries? *Rev. Fish Biol. Fish.* **2017**, *27*, 909–929. [CrossRef]

3. Mondal, S.; Vayghan, A.H.; Lee, M.A.; Wang, Y.C.; Semedi, B. Habitat suitability modeling for the feeding ground of immature albacore in the southern Indian Ocean using satellite-derived sea surface temperature and chlorophyll data. *Remote Sens.* **2021**, *13*, 2669. [[CrossRef](#)]
4. Chen, I.C.; Lee, P.F.; Tzeng, W.N. Distribution of albacore (*Thunnus alalunga*) in the Indian Ocean and its relation to environmental factors. *Fish. Oceanogr.* **2005**, *14*, 71–80. [[CrossRef](#)]
5. Hereher, M.E. Assessment of climate change impacts on sea surface temperatures and sea level rise—The Arabian Gulf. *Climate* **2020**, *8*, 50. [[CrossRef](#)]
6. Ruela, R.; Sousa, M.C.; de Castro, M.; Dias, J.M. Global and regional evolution of sea surface temperature under climate change. *Glob. Planet. Chang.* **2020**, *190*, 103190. [[CrossRef](#)]
7. Wiryawan, B.; Loneragan, N.; Mardhiah, U.; Kleinertz, S.; Wahyuningrum, P.I.; Pingkan, J.; Wildan; Timur, P.S.; Duggan, D.; Yulianto, I. Catch per unit effort dynamic of yellowfin tuna related to sea surface temperature and chlorophyll in Southern Indonesia. *Fishes* **2020**, *5*, 28. [[CrossRef](#)]
8. Jansen, T.; Gislason, H. Temperature affects the timing of spawning and migration of North Sea mackerel. *Cont. Shelf Res.* **2011**, *31*, 64–72. [[CrossRef](#)]
9. Kramer, D.L. Dissolved oxygen and fish behavior. *Environ. Biol. Fishes* **1987**, *18*, 81–92. [[CrossRef](#)]
10. Sear, D.A.; Pattison, I.; Collins, A.L.; Newson, M.D.; Jones, J.I.; Naden, P.S.; Carling, P.A. Factors controlling the temporal variability in dissolved oxygen regime of salmon spawning gravels. *Hydrol. Process.* **2014**, *28*, 86–103. [[CrossRef](#)]
11. Urbina, M.A.; Glover, C.N. Effect of salinity on osmoregulation, metabolism and nitrogen excretion in the amphidromous fish, inanga (*Galaxias maculatus*). *J. Exp. Mar. Biol. Ecol.* **2015**, *473*, 7–15. [[CrossRef](#)]
12. Eddy, F.B.; Chang, Y.J. Effects of salinity in relation to migration and development in fish. In *The Vertebrate Gas Transport Cascade: Adaptations to Environment and Mode of Life*; CRC Press, Inc.: Boca Raton, FL, USA, 1993; pp. 35–42.
13. Ferreira-Martins, D.; Coimbra, J.; Antunes, C.; Wilson, J.M. Effects of salinity on upstream-migrating, spawning sea lamprey, *Petromyzon marinus*. *Conserv. Physiol.* **2016**, *4*, cov064. [[CrossRef](#)] [[PubMed](#)]
14. Reinoso, S.; Mora-Pinargote, J.; Bohórquez-Cruz, M.; Sonneholtzner, S.; Argüello-Guevara, W. Effect of water salinity on embryonic development of longfin yellowtail *Seriola rivoliana* larvae. *Aquac. Res.* **2020**, *51*, 1317–1321. [[CrossRef](#)]
15. Yu, W.; Chen, X.; Liu, L. Synchronous Variations in Abundance and Distribution of *Ommastrephes bartramii* and *Dosidicus gigas* in the Pacific Ocean. *J. Ocean. Univ. China* **2021**, *20*, 695–705. [[CrossRef](#)]
16. Fournier, S.; Lee, T.; Wang, X.; Armitage, T.W.; Wang, O.; Fukumori, I.; Kwok, R. Sea surface salinity as a proxy for Arctic Ocean freshwater changes. *J. Geophys. Res. Ocean.* **2020**, *125*, e2020JC016110. [[CrossRef](#)]
17. Asch, R.G.; Checkley, D.M., Jr. Dynamic height: A key variable for identifying the spawning habitat of small pelagic fishes. *Deep Sea Res. Part I Oceanogr. Res. Pap.* **2013**, *71*, 79–91. [[CrossRef](#)]
18. Ma, T.; Wu, G.; Liu, Y.; Mao, J. Abnormal warm sea-surface temperature in the Indian Ocean, active potential vorticity over the Tibetan Plateau, and severe flooding along the Yangtze River in summer 2020. *Q. J. R. Meteorol. Soc.* **2022**, *148*, 1001–1019. [[CrossRef](#)]
19. Garcia-Soto, C.; Cheng, L.; Caesar, L.; Schmidtko, S.; Jewett, E.B.; Cheripka, A.; Rigor, I.; Caballero, A.; Chiba, S.; Báez, J.C.; et al. An overview of ocean climate change indicators: Sea surface temperature, ocean heat content, ocean pH, dissolved oxygen concentration, Arctic Sea ice extent, thickness and volume, sea level and strength of the AMOC (Atlantic Meridional Overturning Circulation). *Front. Mar. Sci.* **2021**, *8*, 642372.
20. Dinnat, E.P.; Le Vine, D.M.; Boutin, J.; Meissner, T.; Lagerloef, G. Remote sensing of sea surface salinity: Comparison of satellite and in situ observations and impact of retrieval parameters. *Remote Sens.* **2019**, *11*, 750. [[CrossRef](#)]
21. Wells, B.K.; Grimes, C.B.; Waldvogel, J.B. Quantifying the effects of wind, upwelling, curl, sea surface temperature and sea level height on growth and maturation of a California Chinook salmon (*Oncorhynchus tshawytscha*) population. *Fish. Oceanogr.* **2007**, *16*, 363–382. [[CrossRef](#)]
22. Makwinja, R.; Mengistou, S.; Kaunda, E.; Alamirew, T. Lake Malombe fish stock fluctuation: Ecosystem and fisherfolks. *Egypt. J. Aquat. Res.* **2021**, *47*, 321–327. [[CrossRef](#)]
23. Michael-Bitton, G.; Gal, G.; Corrales, X.; Ofir, E.; Shechter, M.; Zemah-Shamir, S. Economic aspects of fish stock accounting as a renewable marine natural capital: The Eastern Mediterranean continental shelf ecosystem as a case study. *Ecol. Econ.* **2022**, *200*, 107539. [[CrossRef](#)]
24. Alqattan, M.E.; Gray, T.S. Marine Pollution in Kuwait and Its Impacts on Fish-Stock Decline in Kuwaiti Waters: Reviewing the Kuwaiti Government's Policies and Practices. *Front. Sustain.* **2021**, *2*, 667822. [[CrossRef](#)]
25. Khoshnood, Z. Effects of environmental pollution on fish: A short review. *Transylv. Rev. Syst. Ecol. Res.* **2017**, *19*, 49–60. [[CrossRef](#)]
26. IPCC. *Climate Change 2013: The Physical Science Basis. Contribution of Working Group I to the Fifth Assessment Report of the Intergovernmental Panel on Climate Change*; Cambridge University Press: Cambridge, UK, 2013.
27. Lønborg, C.; Carreira, C.; Jickells, T.; Álvarez-Salgado, X.A. Impacts of global change on ocean dissolved organic carbon (DOC) cycling. *Front. Mar. Sci.* **2020**, *7*, 466. [[CrossRef](#)]
28. Arneth, A.; Shin, Y.J.; Leadley, P.; Rondinini, C.; Bukvareva, E.; Kolb, M.; Midgley, G.F.; Oberdorff, T.; Palomo, I.; Saito, O. Post-2020 biodiversity targets need to embrace climate change. *Proc. Natl. Acad. Sci. USA* **2020**, *117*, 30882–30891. [[CrossRef](#)]
29. Suh, S.; Johnson, J.A.; Tambjerg, L.; Sim, S.; Broeckx-Smith, S.; Reyes, W.; Chaplin-Kramer, R. Closing yield gap is crucial to avoid potential surge in global carbon emissions. *Glob. Environ. Chang.* **2020**, *63*, 102100. [[CrossRef](#)]

30. Masson-Delmotte, V.; Zhai, P.; Pörtner, H.O.; Roberts, D.; Skea, J.; Shukla, P.R. *Global Warming of 1.5 C: IPCC Special Report on Impacts of Global Warming of 1.5 C above Pre-Industrial Levels in Context of Strengthening Response to Climate Change, Sustainable Development, and Efforts to Eradicate Poverty*; Cambridge University Press: Cambridge, UK, 2022.
31. Kroeker, K.J.; Sanford, E. Ecological leverage points: Species interactions amplify the physiological effects of global environmental change in the ocean. *Annu. Rev. Mar. Sci.* **2022**, *14*, 75–103. [[CrossRef](#)]
32. Hu, W.; Du, J.; Su, S.; Tan, H.; Yang, W.; Ding, L.; Dong, P.; Yu, W.; Zheng, X.; Chen, B. Effects of climate change in the seas of China: Predicted changes in the distribution of fish species and diversity. *Ecol. Indic.* **2022**, *134*, 108489. [[CrossRef](#)]
33. Nataniel, A.; Pennino, M.G.; Lopez, J.; Soto, M. Modelling the impacts of climate change on skipjack tuna (*Katsuwonus pelamis*) in the Mozambique Channel. *Fish. Oceanogr.* **2022**, *31*, 149–163. [[CrossRef](#)]
34. Nicol, S.; Lehodey, P.; Senina, I.; Bromhead, D.; Frommel, A.Y.; Hampton, J.; Havenhand, J.; Margulies, D.; Munday, P.L.; Scholey, V.; et al. Ocean futures for the world's largest yellowfin tuna population under the combined effects of ocean warming and acidification. *Front. Mar. Sci.* **2022**, *9*, 816772. [[CrossRef](#)]
35. Olafsdottir, A.H.; Utne, K.R.; Jacobsen, J.A.; Jansen, T.; Óskarsson, G.J.; Nøttestad, L.; Elvarsson, B.; Broms, C.; Slotte, A. Geographical expansion of Northeast Atlantic mackerel (*Scomber scombrus*) in the Nordic Seas from 2007 to 2016 was primarily driven by stock size and constrained by low temperatures. *Deep. Sea Res. Part II Top. Stud. Oceanogr.* **2019**, *159*, 152–168. [[CrossRef](#)]
36. Rutterford, L.A.; Simpson, S.D.; Bogstad, B.; Devine, J.A.; Genner, M.J. Sea temperature is the primary driver of recent and predicted fish community structure across Northeast Atlantic shelf seas. *Glob. Chang. Biol.* **2023**, *29*, 2510–2521. [[CrossRef](#)] [[PubMed](#)]
37. Issifu, I.; Alava, J.J.; Lam, V.W.; Sumaila, U.R. Impact of ocean warming, overfishing and mercury on European fisheries: A risk assessment and policy solution framework. *Front. Mar. Sci.* **2022**, *8*, 770805. [[CrossRef](#)]
38. Zhu, B.R.; Verhoeven, M.A.; Velasco, N.; Sanchez-Aguilar, L.; Zhang, Z.; Piersma, T. Current breeding distributions and predicted range shifts under climate change in two subspecies of Black-tailed Godwits in Asia. *Glob. Chang. Biol.* **2022**, *28*, 5416–5426. [[CrossRef](#)]
39. Cuilleret, M.; Doyen, L.; Gomes, H.; Blanchard, F. Resilience management for coastal fisheries facing with global changes and uncertainties. *Econ. Anal. Policy* **2022**, *74*, 634–656. [[CrossRef](#)]
40. Yang, W.; Zhang, J.; Krebs, P. Low impact development practices mitigate urban flooding and non-point pollution under climate change. *J. Clean. Prod.* **2022**, *347*, 131320. [[CrossRef](#)]
41. Pilcher, D.J.; Cross, J.N.; Hermann, A.J.; Kearney, K.A.; Cheng, W.; Mathis, J.T. Dynamically downscaled projections of ocean acidification for the Bering Sea. *Deep. Sea Res. Part II Top. Stud. Oceanogr.* **2022**, *198*, 105055. [[CrossRef](#)]
42. Vayghan, A.H.; Poorbagher, H.; Shahraiyini, H.T.; Fazli, H.; Saravi, H.N. Suitability indices and habitat suitability index model of Caspian kutum (*Rutilus frisii kutum*) in the southern Caspian Sea. *Aquat. Ecol.* **2013**, *47*, 441–451. [[CrossRef](#)]
43. Lee, M.A.; Weng, J.S.; Lan, K.W.; Vayghan, A.H.; Wang, Y.C.; Chan, J.W. Empirical habitat suitability model for immature albacore tuna in the North Pacific Ocean obtained using multisatellite remote sensing data. *Int. J. Remote Sens.* **2020**, *41*, 5819–5837. [[CrossRef](#)]
44. Chen, X.; Li, G.; Feng, B.; Tian, S. Habitat suitability index of Chub mackerel (*Scomber japonicus*) from July to September in the East China Sea. *J. Oceanogr.* **2009**, *65*, 93–102. [[CrossRef](#)]
45. Lee, D.; Son, S.; Kim, W.; Park, J.M.; Joo, H.; Lee, S.H. Spatio-temporal variability of the habitat suitability index for Chub Mackerel (*Scomber japonicus*) in the East/Japan Sea and the South sea of South Korea. *Remote Sens.* **2018**, *10*, 938. [[CrossRef](#)]
46. Lee, D.; Son, S.H.; Lee, C.I.; Kang, C.K.; Lee, S.H. Spatio-temporal variability of the habitat suitability index for the *Todarodes pacificus* (Japanese common squid) around South Korea. *Remote Sens.* **2019**, *11*, 2720. [[CrossRef](#)]
47. Poloczanska, E.S.; Brown, C.J.; Sydeman, W.J.; Kiessling, W.; Schoeman, D.S.; Moore, P.J.; Brander, K.; Bruno, J.F.; Buckley, L.B.; Burrows, M.T.; et al. Global imprint of climate change on marine life. *Nat. Clim. Chang.* **2013**, *3*, 919–925. [[CrossRef](#)]
48. Chang, Y.J.; Hsu, J.; Lai, P.K.; Lan, K.W.; Tsai, W.P. Evaluation of the impacts of climate change on albacore distribution in the South Pacific Ocean by using ensemble forecast. *Front. Mar. Sci.* **2021**, *8*, 731950. [[CrossRef](#)]
49. Christian, J.R.; Holmes, J. Changes in albacore tuna habitat in the northeast Pacific Ocean under anthropogenic warming. *Fish. Oceanogr.* **2016**, *25*, 544–554. [[CrossRef](#)]
50. Dell'Apa, A.; Carney, K.; Davenport, T.M.; Carle, M.V. Potential medium-term impacts of climate change on tuna and billfish in the Gulf of Mexico: A qualitative framework for management and conservation. *Mar. Environ. Res.* **2018**, *141*, 1–11. [[CrossRef](#)] [[PubMed](#)]
51. Jones, M.C.; Cheung, W.W. Using fuzzy logic to determine the vulnerability of marine species to climate change. *Glob. Chang. Biol.* **2018**, *24*, e719–e731. [[CrossRef](#)]
52. Beaugrand, G.; Kirby, R.R. How do marine pelagic species respond to climate change? Theories and observations. *Annu. Rev. Mar. Sci.* **2018**, *10*, 169–197. [[CrossRef](#)]
53. Oschlies, A. *Ocean Deoxygenation from Climate Change*; IUCN: Gland, Switzerland, 2019.
54. Bromhead, D.; Scholey, V.; Nicol, S.; Margulies, D.; Wexler, J.; Stein, M.; Hoyle, S.; Lennert-Cody, C.; Williamson, J.; Havenhand, J.; et al. The potential impact of ocean acidification upon eggs and larvae of yellowfin tuna (*Thunnus albacares*). *Deep Sea Res. Part II Top. Stud. Oceanogr.* **2015**, *113*, 268–279. [[CrossRef](#)]
55. Olson, S.; Jansen, M.F.; Abbot, D.S.; Halevy, I.; Goldblatt, C. The effect of ocean salinity on climate and its implications for Earth's habitability. *Geophys. Res. Lett.* **2022**, *49*, e2021GL095748. [[CrossRef](#)]

56. Sagarminaga, Y.; Arrizabalaga, H. Relationship of Northeast Atlantic albacore juveniles with surface thermal and chlorophyll-a fronts. *Deep. Sea Res. Part II Top. Stud. Oceanogr.* **2014**, *107*, 54–63. [[CrossRef](#)]
57. Arrizabalaga, H.; Dufour, F.; Kell, L.; Merino, G.; Ibaibarriaga, L.; Chust, G.; Irigoien, X.; Santiago, J.; Murua, H.; Fraile, I.; et al. Global habitat preferences of commercially valuable tuna. *Deep. Sea Res. Part II Top. Stud. Oceanogr.* **2015**, *113*, 102–112. [[CrossRef](#)]
58. Rowden, A.A.; Anderson, O.F.; Georgian, S.E.; Bowden, D.A.; Clark, M.R.; Pallentin, A.; Miller, A. High-resolution habitat suitability models for the conservation and management of vulnerable marine ecosystems on the Louisville Seamount Chain, South Pacific Ocean. *Front. Mar. Sci.* **2017**, *4*, 335. [[CrossRef](#)]
59. Mugagga, F.; Nabaasa, B.B. The centrality of water resources to the realization of Sustainable Development Goals (SDG). A review of potentials and constraints on the African continent. *Int. Soil Water Conserv. Res.* **2016**, *4*, 215–223. [[CrossRef](#)]
60. Ntona, M.; Morgera, E. Connecting SDG 14 with the other Sustainable Development Goals through marine spatial planning. *Mar. Policy* **2018**, *93*, 214–222. [[CrossRef](#)]
61. Virto, L.R. A preliminary assessment of the indicators for Sustainable Development Goal (SDG) 14 “Conserve and sustainably use the oceans, seas and marine resources for sustainable development”. *Mar. Policy* **2018**, *98*, 47–57. [[CrossRef](#)]
62. Kenny, A.J.; Campbell, N.; Koen-Alonso, M.; Pepin, P.; Diz, D. Delivering sustainable fisheries through adoption of a risk-based framework as part of an ecosystem approach to fisheries management. *Mar. Policy* **2018**, *93*, 232–240. [[CrossRef](#)]
63. Cormier, R.; Elliott, M. SMART marine goals, targets and management—Is SDG 14 operational or aspirational, is ‘Life Below Water’ sinking or swimming? *Mar. Pollut. Bull.* **2017**, *123*, 28–33. [[CrossRef](#)] [[PubMed](#)]

Disclaimer/Publisher’s Note: The statements, opinions and data contained in all publications are solely those of the individual author(s) and contributor(s) and not of MDPI and/or the editor(s). MDPI and/or the editor(s) disclaim responsibility for any injury to people or property resulting from any ideas, methods, instructions or products referred to in the content.